ACTIVE CONTROL OF TURBULENT FLOW OVER A MODEL VEHICLE FOR DRAG REDUCTION

Haecheon Choi[1,2,3], Jeonglae Kim[1], Seonghyeon Hahn[2], Dong-kon Lee[1], Jin Choi[1], Woo-Pyung Jeon[2]
[1]School of Mechanical and Aerospace Engineering
Seoul National University
Seoul 151–742, Korea
[2]Center for Turbulence and Flow Control Research
Institute of Advanced Machinery and Design
Seoul National University
Seoul 151–742, Korea
[3]Corresponding author: choi@socrates.snu.ac.kr

ABSTRACT

The objectives of the present study are to examine the applicability of the distributed forcing (Kim and Choi 2002) to flows over bluff bodies having a fixed separation and thus to evaluate the universality of the distributed forcing. Therefore, both the large eddy simulation (LES) with a dynamic model for subgrid-scale stress components and wind-tunnel experiment are carried out for flow over a model vehicle. LES is performed at the Reynolds number of $\mathrm{Re} = u_\infty h/\nu = 4200$, whereas two different Reynolds numbers of $\mathrm{Re} = 20,000$ and $40,000$ are considered in the experiment, where u_∞ is the free-stream velocity and h is the body height. In LES at $\mathrm{Re} = 4200$, a significant amount of the base-pressure recovery is obtained with the in-phase distributed forcing, while the out-of-phase one leaves the base pressure almost unchanged. Furthermore, the in-phase distributed forcing substantially suppresses vortex shedding, whereas the out-of-phase one does not seem to influence vortex shedding very much. The power spectra of the velocity fluctuations and the spatial distribution of the Reynolds shear stress also show that the in-phase distributed forcing considerably enhances the three dimensionality of the wake behind the model vehicle. Similar results are also obtained from the in-phase forcing in the experiment at higher Reynolds numbers and thus it is believed that the distributed forcing is applicable to a broad class of two-dimensional bluff bodies for drag reduction in a wide range of the Reynolds number.

INTRODUCTION

Development of an efficient high-speed transportation vehicle is one of the most important applications in turbulence control for drag reduction. Up to now, attempts to control turbulent wakes behind bluff bodies for drag reduction have been mostly performed for flow over a circular cylinder due to its geometric simplicity. However, for large-scale transportation vehicles such as buses and trucks, the separation point is fixed at the trailing edge due to their blunt shape near the base surface. In this case, the flow changes suddenly near the trailing edge from a flat-plate boundary layer flow to a wake. This flow pattern should be considered in order to develop a new efficient control method of achieving a significant drag reduction.

So far, control of flow over a bluff body with a blunt trailing edge and thus having a fixed separation has been investigated mainly by experiments conducted with a model vehicle. Bearman (1965) obtained the recovery of the base pressure by using a splitter plate, which significantly retards the interaction between the vortices generated at the upper and lower edges of the model vehicle. On the other hand, Tanner (1972), Petrusma and Gai (1994) and Tombazis and Bearman (1997) reported the suppression of the Kármán vortex shedding and the base-pressure recovery up to 60% by modifying the shape of the blunt trailing edge in the spanwise direction. In addition to these studies on passive control strategies, some researchers also investigated simple non-feedback active control methods such as the base bleed or base suction (Wood 1964; Bearman 1967; Yao and Sandham 1999). However, the methods mentioned above are somewhat impractical or inefficient to be directly applied to large-scale transportation vehicles in that the entire shape of the base surface should be modified and that control input should be imposed on the flow after separation.

Recently, Kim and Choi (2002) has developed a new active open-loop control method, named distributed forcing, for reducing drag on a circular cylinder and showed a significant drag reduction for laminar and turbulent flows behind the cylinder. This method has been found to introduce three-dimensional disturbances to the flow behind a circular cylinder and efficiently alter the two-dimensional wake characteristics. Therefore, the objectives of the present study are to examine the applicability of the distributed forcing to the wake behind a bluff body having a fixed separation and to evaluate the universality of the distributed forcing.

TOOLS

In order to assess the applicability of the distributed forcing to flow over a bluff body having a fixed separation in a wide range of the Reynolds number, both the large eddy simulation (LES) and wind-tunnel experiment are carried out for flow over a model vehicle in the present study. The main aim of LES in the present study is to understand the flow change. Details on the computation and experiment are briefly summarized in this section.

Computational Details

Large eddy simulation with a dynamic model for subgrid-scale stress components (Germano *et al.* 1991; Lilly 1992)

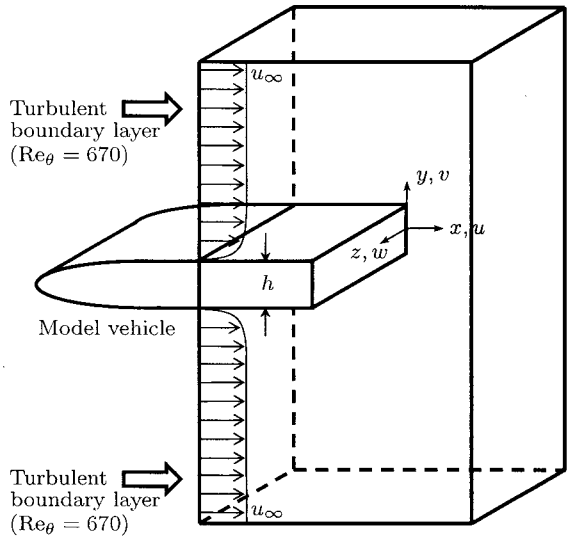

Figure 1: Schematic diagram of the computational domain.

is carried out for flow over a model vehicle at the Reynolds number of Re $= u_\infty h/\nu = 4200$, where u_∞ is the free-stream velocity and h is the body height. Figure 1 shows the schematic diagram of the computational domain. In LES, only the flow field over the rear part of the model vehicle is chosen to be simulated in a Cartesian coordinate system with a turbulent boundary layer flow of $\mathrm{Re}_\theta = u_\infty \theta/\nu = 670$ (θ is the momentum thickness) introduced at the domain inlet, instead of the entire flow field around a model vehicle. Note that the ratio of the thickness of the boundary layer (δ) entering the domain inlet to the body height is quite large ($\delta/h \approx 1.4$) in the present configuration. Since the nose section of the model vehicle is not included in our numerical simulation, direct measurement of drag is not possible and thus drag increase or decrease is assessed rather indirectly by the recovery of the base pressure.

The size of the computational domain is $-3 < x/h < 15$, $-28 < y/h < 28$ and $0 < z/h < 4$ and the number of grid points is $340 \times 240 \times 64$ in the streamwise, transverse and spanwise directions, respectively. The no-slip boundary condition is imposed at the body surface, while the boundary conditions of $u = u_\infty$ and $\partial v/\partial y = \partial w/\partial y = 0$ are imposed at the far-field boundary. The convective outflow boundary condition is used at the domain outlet and the periodic boundary condition is imposed in the spanwise direction. The computation is carried out with the fixed computational time step of $\Delta t u_\infty/h = 0.019$.

Experimental Setup

The experiment is conducted in an open-type wind tunnel. The nose of the model vehicle is shaped into a half ellipse with its ratio of the major to minor axis of 8, following Tombazis and Bearman (1997). Sizes of the model vehicle and the test section are 380mm (x)×60mm (y)×300mm (z) and 3m (x)×0.6m (y)×0.3m (z), respectively. Trip wires are located at the 100mm downstream location from the nose of the model vehicle. Two different free-stream velocities of u_∞ = 5m/s and 10m/s are considered in the experiment and the corresponding Reynolds numbers are Re = 20,000 and 40,000, respectively.

The base pressure is measured by 220CD manometers through the pressure holes established along the centerline of the base surface ($y = 0$). Flow visualization is also carried out using smoke wires, where RP-1 fog fluid of Red Point Inc. and 5W argon laser are used for smoke-generating material and a light source, respectively. The exposure time for a digital camera is set to be 1/45 second.

DISTRIBUTED FORCING

Figure 2 shows the schematic diagram of the distributed forcing. Distributed forcing is composed of spanwisely sinusoidal but temporally steady blowing and suction applied on both the upper and lower body surfaces at the trailing edge of the model vehicle:

$$\Phi(z) = \Phi_{max} \sin(2\pi \frac{z}{\lambda_z}) \qquad (1)$$

Here, Φ, Φ_{max} and λ_z denote the control input, amplitude and wavelength of the blowing/suction, respectively.

In LES, the forcing amplitude is set to be $\Phi_{max} = 0.1 u_\infty$ and the forcing wavelength is chosen to be $\lambda_z = 4h$. This wavelength is chosen because the control performance is best at $\lambda_z = 3 \sim 4d$ (d is the cylinder diameter) in flow over a circular cylinder (Kim and Choi 2002). The forcing angle and the slot width are fixed to be $\beta = 45°$ and $b = 0.1h$, respectively. On the other hand, two different types of the distributed forcing are considered (Figs. 2b and 2c): the phase difference between the forcing velocities from upper and lower surfaces is zero (in-phase) or π (out-of-phase).

In the experiment, only the in-phase distributed forcing is applied. The in-phase forcing is embodied in the present experiment by making slits at upper and lower trailing edges and operating a series of fans established inside the model vehicle with their wind directions changed alternately along the spanwise direction. Each fan is driven by the voltage of 18V and the maximum velocity from the slit amounts to 4.1m/s with fans operated without the freestream. In the experiment, the forcing wavelength is fixed to be $\lambda_z \approx 2h$.

RESULTS AND DISCUSSION

LES at Re=4200

Figure 3 shows the distribution of the base-pressure coefficient (C_{pb}) along the centerline of the base surface (i.e. $y = 0$). The base pressure is recovered by about 30% with the in-phase distributed forcing, which implies a large amount of drag reduction. On the other hand, the out-of-phase one leaves the base pressure almost unchanged as compared to that of the uncontrolled flow, which is quite similar to the result observed in flow over a circular cylinder at $\mathrm{Re}_d = 100$ (Kim and Choi 2002). It is also notable that the in-phase forcing yields a substantial amount of the base-pressure recovery over the entire span of the base surface, although it considerably activates three-dimensional motions in the wake (see below).

Figure 4 shows instantaneous vortical structures for the uncontrolled and controlled cases using the method of λ_2 by Jeong and Hussain (1995). A typical Kármán vortex shedding is clearly observed in the uncontrolled flow and it is obvious that the in-phase distributed forcing substantially suppresses vortex shedding. Furthermore, the naturally occurring vortices right behind the body certainly disappear with the in-phase forcing, which seems to be the main reason for the substantial amount of the base-pressure recovery. This flow pattern is also quite similar to that from the in-phase controlled flow field behind a circular cylinder at

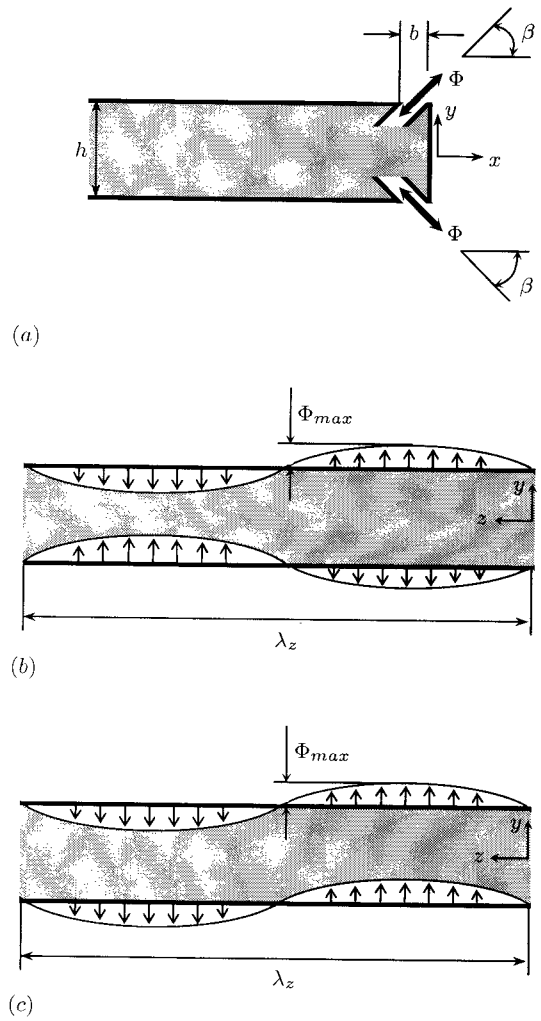

Figure 2: Schematic diagram of the distributed forcing: (*a*) side view; (*b*) front view of the in-phase forcing; (*c*) front view of the out-of-phase forcing.

$\mathrm{Re}_d = 3900$ (Kim and Choi 2002). On the other hand, the out-of-phase one does not seem to influence vortex shedding. We conjecture that the control performance of the out-of-phase forcing is closely associated with the boundary layer thickness relative to the size of a bluff body. For example, in the study on flow over a circular cylinder by Kim and Choi (2002), the boundary layer on the cylinder surface is quite thick ($\delta/d \approx 0.28$) at $\mathrm{Re}_d = 100$ and the out-of-phase forcing neither affects the flow field nor reduces drag at that Reynolds number. However, at $\mathrm{Re}_d = 3900$, the boundary layer becomes thinner ($\delta/d \approx 0.07$) and the shear layer formed right behind the cylinder becomes more susceptible to external disturbances. Therefore, a certain amount of drag reduction could be obtained even with the out-of-phase forcing in that case. In the present configuration of flow over a model vehicle, the boundary layer is also quite thick as compared to the body height ($\delta/h \approx 1.4$) and thus the out-of-phase forcing does not work.

Tombazis and Bearman (1997) reported that the detected frequency varies in the spanwise direction when three-dimensional motions are activated in the wake. Figure 5 shows the energy spectra of the transverse velocity fluctuations measured at $(x/h, y/h) = (3, 0)$ and $z = \lambda_z/4$, $\lambda_z/2$ and $3\lambda_z/4$. For the uncontrolled flow, there appears a sharp

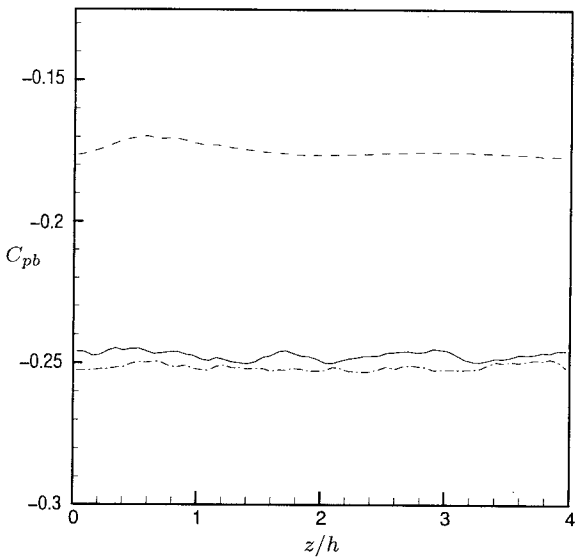

Figure 3: Distribution of the base-pressure coefficient along the centerline of the base surface at Re = 4200: ———, uncontrolled flow; – – – –, in-phase forcing; —·—, out-of-phase forcing.

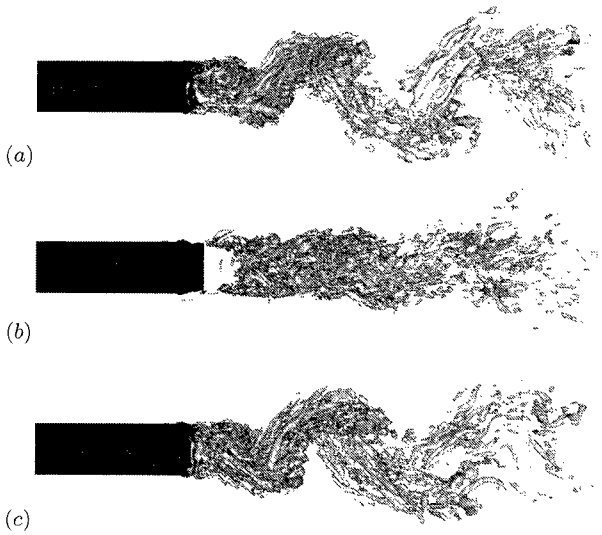

Figure 4: Vortical structures at Re = 4200: (*a*) uncontrolled flow; (*b*) in-phase forcing; (*c*) out-of-phase forcing.

peak in the energy spectra at all the spanwise locations which corresponds to the vortex shedding frequency. The dominant frequency does not vary in the spanwise direction and thus vortex shedding is completely two-dimensional for the uncontrolled flow. On the other hand, the maximum values in the energy spectra are significantly decreased by the in-phase distributed forcing, which again confirms the substantial suppression of vortex shedding. In addition, the dominant frequency becomes higher at the location of maximum suction ($z = 3\lambda_z/4$) than at the location of maximum blowing ($z = \lambda_z/4$), indicating that vortex shedding becomes three-dimensional with the in-phase distributed forcing and that the complete modification of the wake structure with the in-phase forcing shown in figure 4(*b*) may be related to the enhancement of the three dimensionality. Meanwhile, the out-of-phase forcing has no influence on the vortex shed-

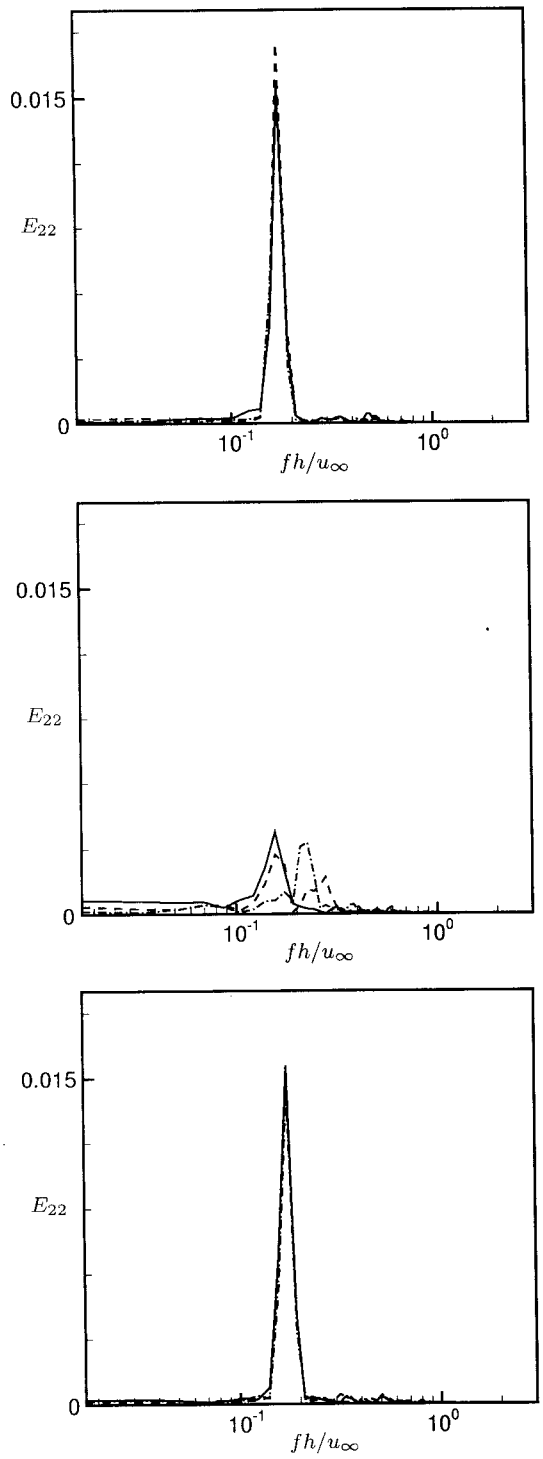

Figure 5: Energy spectra of the transverse velocity fluctuations at $(x/h, y/h) = (3, 0)$ for the uncontrolled (top), in-phase controlled (middle) and out-of-phase controlled (bottom) flows (Re = 4200): ———, $z = \lambda_z/4$; – – – –, $z = \lambda_z/2$; —·—, $z = 3\lambda_z/4$.

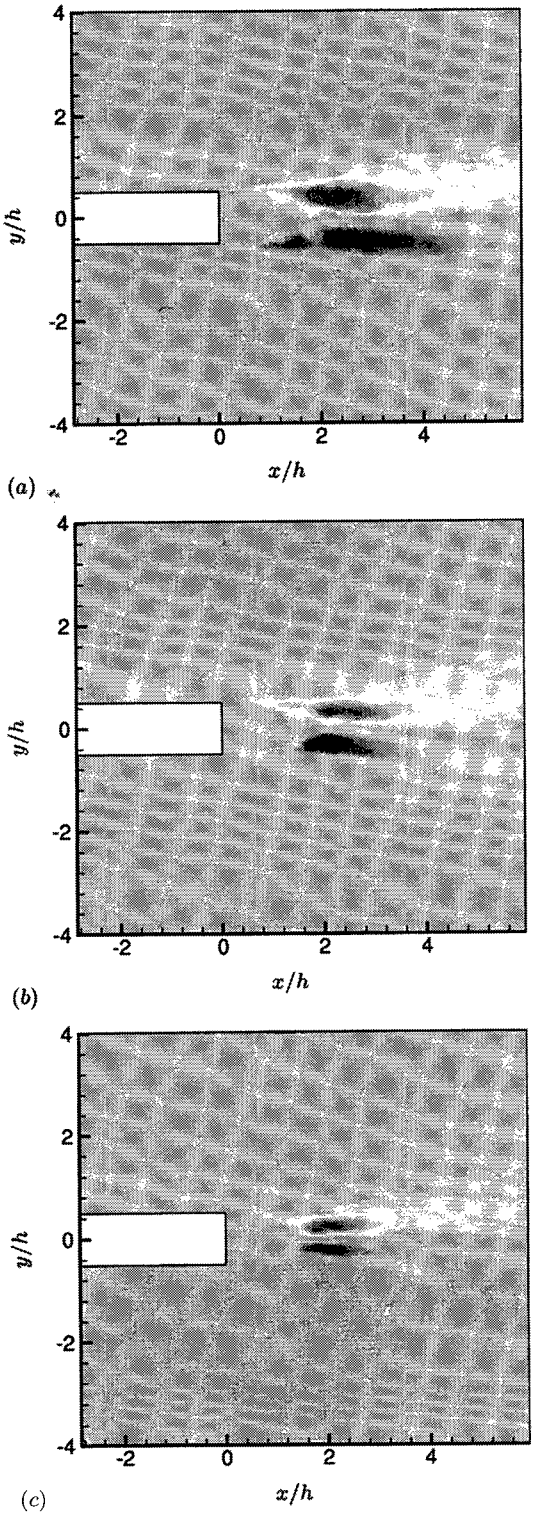

Figure 6: Contours of the Reynolds shear stress with the in-phase forcing at Re = 4200: (*a*) $z = \lambda_z/4$ (maximum blowing location); (*b*) $z = \lambda_z/2$ (zero forcing location); (*c*) $z = 3\lambda_z/4$ (maximum suction location).

ding frequency.

The activation of three-dimensional motions with the in-phase distributed forcing is also observed in turbulence quantities. Figure 6 shows contours of the Reynolds shear stress ($-\overline{u'v'}$) at $z = \lambda_z/4$, $\lambda_z/2$ and $3\lambda_z/4$ with the in-phase distributed forcing. The Reynolds shear stress with the in-phase forcing varies significantly in the spanwise direction. It increases at the location of maximum blowing ($z = \lambda_z/4$) but substantially decreases at the location of maximum suction ($z = 3\lambda_z/4$) due to the stabilization effect. As is expected, the out-of-phase forcing did not alter the distribution of the Reynolds shear stress (not shown here).

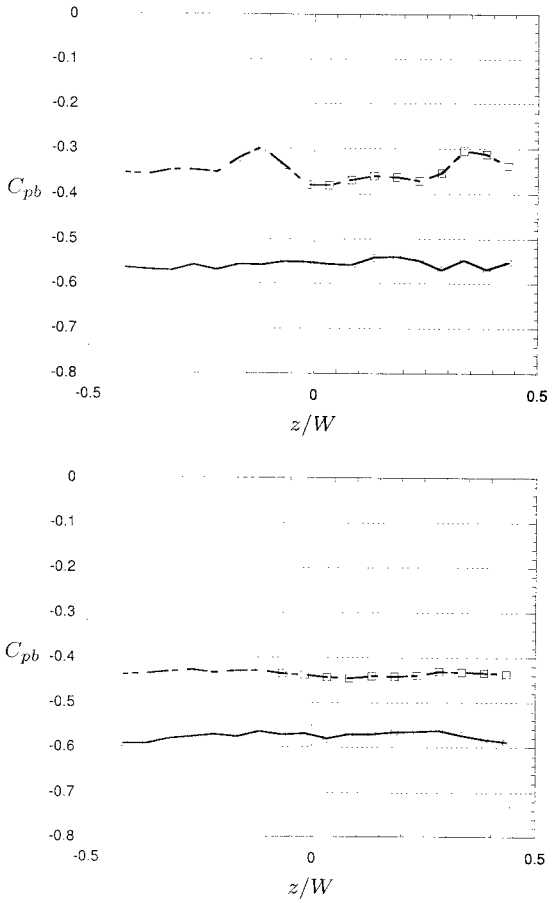

Figure 7: Distribution of the base-pressure coefficient along the centerline of the base surface at Re = 20,000 (top) and 40,000 (bottom): ———, uncontrolled flow; — — —, in-phase forcing. W denotes the spanwise size of the model vehicle.

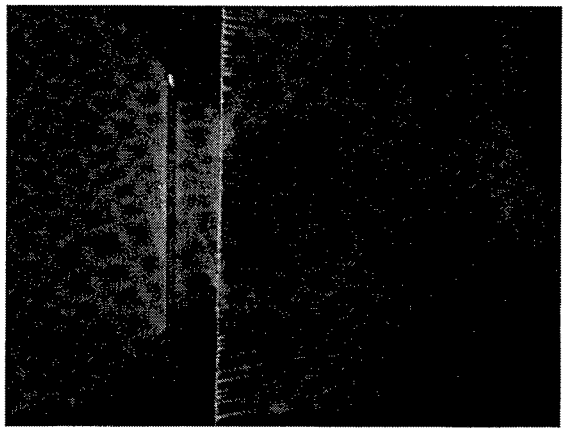

(a)

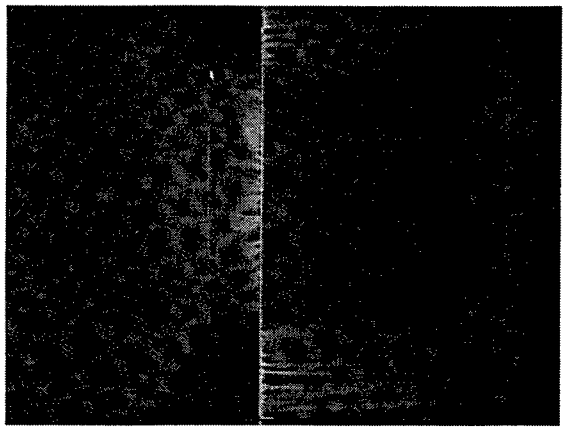

(b)

Figure 8: Smoke-wire visualization at Re = 20,000 near the location of maximum blowing: (a) uncontrolled flow; (b) in-phase forcing. The flow direction is from left to right. Here, the smoke wire is located along the y direction.

Similar behaviors are also found in other turbulence quantities.

Experiment at Re=20,000 and 40,000

Figure 7 shows the distribution of the base-pressure coefficient along the centerline of the base surface at Re = 20,000 and 40,000. As was observed in LES at Re = 4200 (figure 3), a substantial amount of the base-pressure recovery is also obtained with the in-phase distributed forcing at these higher Reynolds numbers and the percentages of base-pressure recovery amount to about 35% and 22% at Re = 20,000 and 40,000, respectively. Therefore, the distributed forcing is believed to be an effective control method applicable to a wide range of the Reynolds number. With the in-phase forcing, the base-pressure is recovered more at the blowing location ($z/W = -0.12$ and 0.35) than at the suction location ($z/W = -0.3$ and 0.15) because blowing pushes the low-pressure region away from the base surface, but the spanwise variation of the base pressure becomes milder at Re = 40,000 as the ratio of the blowing/suction magnitude to the free-stream velocity becomes small.

Figures 8 and 9 show a flow visualization using smoke wires at Re = 20,000 near the locations of maximum blowing and maximum suction, respectively. It is clearly shown that the in-phase distributed forcing remarkably influences the wake structure near the base surface. The wake vortex formed right near the base surface is pushed downstream at the maximum blowing location (Fig. 8), while the size of the recirculation bubble is significantly reduced near the maximum suction location (Fig. 9).

CONCLUSION

In order to examine the applicability of the distributed forcing (Kim and Choi 2002) to flow over a bluff body having a fixed separation and thus to evaluate the universality of the distributed forcing, both the large eddy simulation (LES) with a dynamic model for subgrid-scale stress components and wind-tunnel experiment were carried out for flow over a model vehicle in the present study. LES was performed at the Reynolds number of Re = 4200, whereas two different Reynolds numbers of Re = 20,000 and 40,000 were considered in the experiment. In LES at Re = 4200, a significant amount of the base-pressure recovery was obtained with the in-phase distributed forcing, while the out-of-phase one left the base pressure almost unchanged. Furthermore, the in-phase distributed forcing substantially suppressed vortex shedding, whereas the out-of-phase one did not seem to influence vortex shedding. The in-phase distributed forcing considerably enhanced the three dimensionality of the wake behind the model vehicle. Similar results were also obtained with the in-phase forcing in the experiment at higher

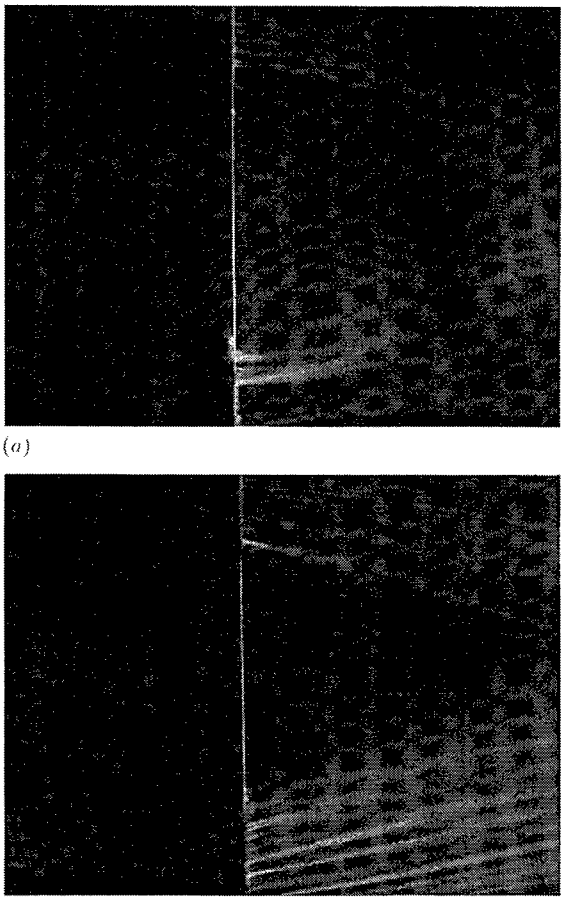

(a)

(b)

Figure 9: Smoke-wire visualization at Re = 20,000 near the location of maximum suction: (a) uncontrolled flow; (b) in-phase forcing. The flow direction is from left to right. Here, the smoke wire is located along the y direction.

Reynolds numbers. We believe that the distributed forcing is applicable to a broad class of two-dimensional bluff bodies for drag reduction in a wide range of the Reynolds number.

ACKNOWLEDGEMENT

Financial support from the Creative Research Initiatives through the Korean Ministry of Science and Technology is gratefully acknowledged.

REFERENCES

Bearman, P. W., 1965, "Investigation of the flow behind a two-dimensional model with a blunt trailing edge and fitted with splitter plates," *Journal of Fluid Mechanics*, Vol. 21, p. 241.

Bearman, P. W., 1967, "The effect of base bleed on the flow behind a two-dimensional model with a blunt trailing edge," *The Aeronautical Quarterly*, Vol. 18, p. 207.

Germano, M., Piomelli, U., Moin, P. and Cabot, W. H., 1991, "A dynamic subgrid-scale eddy viscosity model," *Physics of Fluids* A, Vol. 3, p. 1760.

Jeong, J. and Hussain, F., 1995, "On the identification of a vortex," *Journal of Fluid Mechanics*, Vol. 285, p. 69.

Kim, J., and Choi, H., 2002, "Distributed forcing of flow over a circular cylinder," *Proceedings, 5th JSME–KSME Fluids Engineering Conference*, Nov. 17–21, Nagoya, Japan.

Lilly, D. K., 1992, "A proposed modification of the Germano subgrid-scale closure method," *Physics of Fluids* A, Vol. 4, p. 633.

Petrusma, M. S. and Gai, S. L., 1994, "The effect of geometry on the base pressure recovery of the segmented blunt trailing edge," *The Aeronautical Journal*, Vol. 98, p. 267.

Tanner, M., 1972, "A method of reducing the base drag of wings with blunt trailing edges," *The Aeronautical Quarterly*, Vol. 23, p. 15.

Tombazis, N., and Bearman, P. W., 1997, "A study of three-dimensional aspects of vortex shedding from a bluff body with a mild geometric disturbance," *Journal of Fluid Mechanics*, Vol. 330, p. 85.

Wood, C. J., 1964, "The effect of base bleed on a periodic wake," *Journal of Royal Aeronautical Society*, Vol. 68, p. 477.

Yao, Y. F. and Sandham, N. D., 1999, "Direct numerical simulation of turbulent trailing-edge flow with base suction/blowing," *AIAA Paper* 99-3406.